A pulmonary vein atlas for radiotherapy planning

Walls, G. M., McCann, C., Ball, P., Atkins, K. M., Mak, R. H., Bedair, A., O'Hare, J., McAleese, J., Harrison, C., Tumelty, K. A., Crockett, C., Black, S.-L., Nelson, C., O'Connor, J., Hounsell, A. R., McGarry, C. K., Butterworth, K. T., Cole, A. J., Jain, S., & Hanna, G. G. (2023). A pulmonary vein atlas for radiotherapy planning. *Radiotherapy and Oncology*, *184*, Article 109680. https://doi.org/10.1016/j.radonc.2023.109680

Published in:
Radiotherapy and Oncology

Document Version:
Publisher's PDF, also known as Version of record

Radiotherapy and Oncology 184 (2023) 109680

Contents lists available at ScienceDirect

Radiotherapy and Oncology

journal homepage: www.thegreenjournal.com

Original Article

A pulmonary vein atlas for radiotherapy planning

Gerard M Walls [a,b,*], Conor McCann [c], Peter Ball [d], Katelyn M Atkins [e], Raymond H Mak [f], Ahmed Bedair [g], Jolyne O'Hare [a], Jonathan McAleese [a], Claire Harrison [a], Karen A Tumelty [a], Cathryn Crockett [a], Sarah-Louise Black [a], Catherine Nelson [a], John O'Connor [b], Alan R Hounsell [a,b], Conor K McGarry [a,b], Karl T Butterworth [b], Aidan J Cole [a,b], Suneil Jain [a,b,1], Gerard G Hanna [a,b,1]

[a] Cancer Centre Belfast City Hospital, Belfast Health & Social Care Trust, Lisburn Road, Belfast, UK; [b] Patrick G Johnston Centre for Cancer Research, Queen's University Belfast, Lisburn Road, Belfast, UK; [c] Department of Cardiology, Belfast City Hospital, Belfast Health & Social Care Trust, Lisburn Road, Belfast, UK; [d] Department of Radiology, Royal Victoria Hospital, Belfast Health & Social Care Trust, 274 Grosvenor Rd, Belfast, UK; [e] Department of Radiation Oncology, Cedars-Sinai Medical Center, Los Angeles, California, USA; [f] Department of Radiation Oncology, Dana-Farber Cancer Institute and Brigham and Women's Hospital, Boston, Massachusetts, USA; [g] North West Cancer Centre, ltnagelvin Hospital, Glenshane Road, Derry, UK

ARTICLE INFO

Article history:
Received 19 September 2022
Received in revised form 10 April 2023
Accepted 19 April 2023
Available online 25 April 2023

Keywords:
Radiation cardiotoxicity
Pulmonary veins
Lung cancer
Cardio-oncology
Atrial fibrillation
Oesophageal cancer

ABSTRACT

Background and Purpose: Cardiac arrhythmia is a recognised potential complication of thoracic radiotherapy, but the responsible cardiac substructures for arrhythmogenesis have not been identified. Arrhythmogenic tissue is commonly located in the pulmonary veins (PVs) of cardiology patients with arrhythmia, however these structures are not currently considered organs-at-risk during radiotherapy planning. A standardised approach to their delineation was developed and evaluated.

Materials and Methods: The gross and radiological anatomy relevant to atrial fibrillation was derived from cardiology and radiology literature by a multidisciplinary team. A region of interest and contouring instructions for radiotherapy computed tomography scans were iteratively developed and subsequently evaluated. Radiation oncologists (n = 5) and radiation technologists (n = 2) contoured the PVs on the four-dimensional planning datasets of five patients with locally advanced lung cancer treated with 1.8–2.75 Gy fractions. Contours were compared to reference contours agreed by the researchers using geometric and dosimetric parameters.

Results: The mean dose to the PVs was 35% prescription dose. Geometric and dosimetric similarity of the observer contours with reference contours was fair, with an overall mean Dice of 0.80 ± 0.02. The right superior PV (mean DSC 0.83 ± 0.02) had better overlap than the left (mean DSC 0.80 ± 0.03), but the inferior PVs were equivalent (mean DSC of 0.78). The mean difference in mean dose was 0.79 Gy ± 0.71 (1.46% ± 1.25).

Conclusion: A PV atlas with multidisciplinary approval led to reproducible delineation for radiotherapy planning, supporting the utility of the atlas in future clinical radiotherapy cardiotoxicity research encompassing arrhythmia endpoints.

Arrhythmia has been recognised as a potential adverse effect of incidental cardiac irradiation during treatment of intrathoracic tumors, such as lung and oesophageal cancer (1–6). Counter to the body of literature that posits cardiotoxicity as a late radiation effect, the latency period for developing arrhythmia in 10% of patients can be shorter than 6 months (2). The most common rhythm disturbance presenting to general cardio-oncology clinics are the atrial tachyarrhythmias, such as atrial fibrillation (AF), where the cardiac cycle is irregular and accelerated (7). Lung and oesophageal cancer are most commonly associated with AF, due to elevated rates of baseline cardiovascular disease, and the complex surgery involved for select cases (8–10).

The aetiology of AF commonly involves abnormal heart muscle where the pulmonary veins (PVs) join the left atrium (LA) (11,12). The PVs are tubular structures whose primary function is to provide passageway for newly oxygenated blood back from the lungs to the heart. The myocardial sleeve is a short and thin extension of atrial cardiac muscle embedded in the wall of the adjoining proximal PV (13,14). In AF, damaged tissue within the myocardial sleeve causes altered propagation of electrical potentials locally leading to abnormal conduction throughout both atria, and subsequently is transmitted to the ventricles.

* Corresponding author at: Patrick G Johnston Centre for Cancer Research, Queen's University Belfast, Lisburn Road, Belfast BT9 7AB, UK.
E-mail address: g.walls@qub.ac.uk (G.M Walls).
[1] these authors contributed equally.

https://doi.org/10.1016/j.radonc.2023.109680
0167-8140/

As radiotherapy is known to cause fibrosis of the cardiac structures, it is plausible that incidental dose deposited in the myocardial sleeves of the PVs during radical thoracic treatment may explain high rates of new arrhythmia during follow-up (15). A radiation dose response not been established for the PVs however, and these vessels have not been included in published cardiac atlas' to date (16–20). A standardised definition for delineation of the PVs will be important for investigators seeking to establish safe dose constraints for these structures. In this study, a multidisciplinary group was formed with the aim of producing recommendations on how the PVs should be contoured by researchers exploring methods of reducing cardiotoxicity in patients undergoing thoracic irradiation.

Materials & methods

Atlas development

A multidisciplinary group of clinicians consisting of a clinical oncologist (GW), a cardiologist (CM) and a thoracic radiologist (PB) was formed with the goal of devising guidance for delineation of the PVs on radiotherapy planning computed tomography (CT). The impetus for this work arose from the observation of a high rate of AF following curative-intent radiotherapy amongst lung cancer cases. AF is common in populations with cardiovascular risk factors, and as a secondary phenomenon due to physiological stresses, including common complications of cancer treatment such as sepsis, however the potential role of the PVs has not been examined. As abnormal tissue at the PV junction with the LA is the target for electrophysiology cardiologists that deliver radiofrequency ablation for refractory AF, it is plausible that radiation-related tissue changes at this region are implicated in the development of AF. The LA-junction region of the PV is relevant specifically as the myocardial tissue of the atrial wall blends with the vascular tissue of the adjoining vein and is susceptible to arrhythmogenic pathophysiology, known as the myocardial sleeve. Therefore, the myocardial sleeve portion of the PVs behave as the organs-at-risk (OARs), although they are referred to as the pulmonary veins throughout as these are what are visible on CT.

Peer-reviewed articles detailing the cardiac histology, radiology and pathophysiology relevant to AF were discussed by the group to develop core principles for the atlas. A step-by-step contouring guideline was then derived based on these discussions, and subsequently modified based on written feedback from external peer review by two radiation oncologists with significant experience in cardiac contouring (KA, RM). Finally, the accessibility of the atlas was independently assessed by two clinical oncologists from two separate cancer centres (AB, JOH) hitherto uninvolved with the project. In designing a pragmatic atlas for delineation of the PVs it is hoped that the relationship of dose to these structures and the onset of AF after thoracic radiotherapy can be systemically investigated in large numbers of patients by multiple centres. Confirmation of this association would provide the stimulus for developing safe dose constraints to minimise the risk of AF after thoracic radiotherapy treatment.

Atlas description

The pulmonary veins join the left atrium (LA) posterolaterally at oblique angles, as shown in Fig. 1. In normal anatomy there are two right-sided and two left-sided veins; a superior vein and an inferior vein. Away from the heart, the two superior veins course anteriorly, where the two inferior veins course posteriorly. The superior and inferior veins can have a region in common prior to where they join the LA, more frequently observed on the left side. Each of the four PVs have distinct geometric features, and there is also large intra-patient variation in anatomical vein shape and size. Furthermore, other anomalies such as the presence of a unilateral additional vein, are not uncommon.

As the course of the anatomical veins is non-uniform and largely in the coronal plane, their shape on axial imaging can vary considerably, ranging from circular, to ovoid, rectangular, sinu-

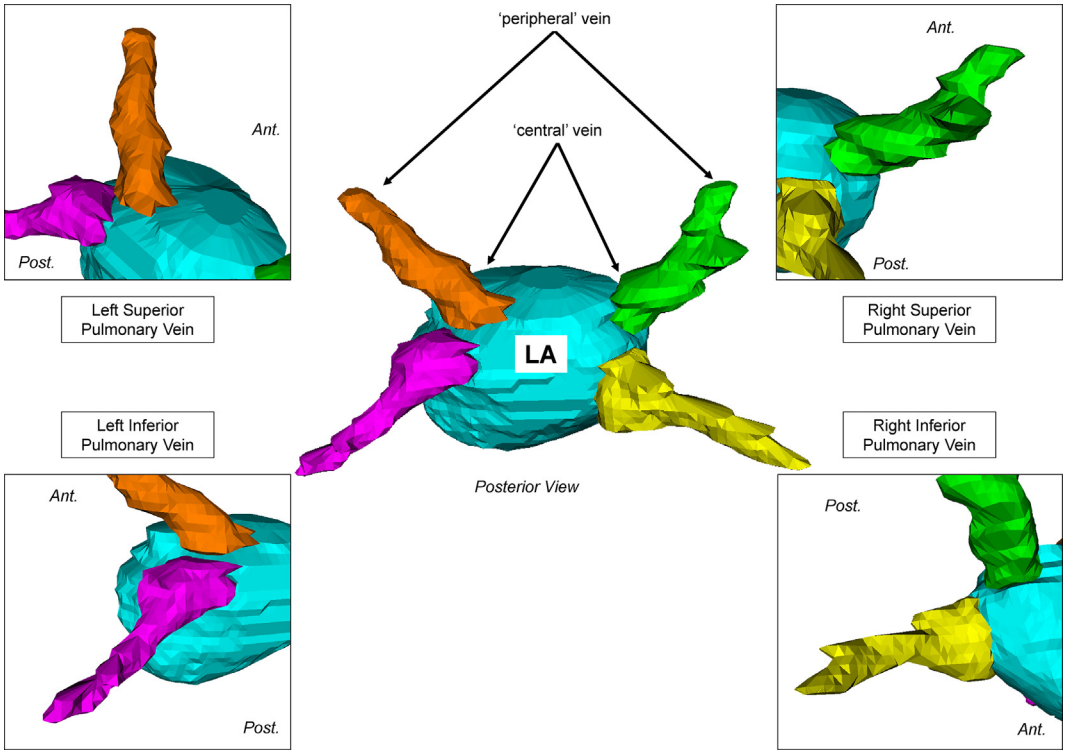

Fig. 1. Three-dimensional re-construction of the anatomy of the pulmonary veins and left atrium from the posterior perspective *(LA = left atrium)*.

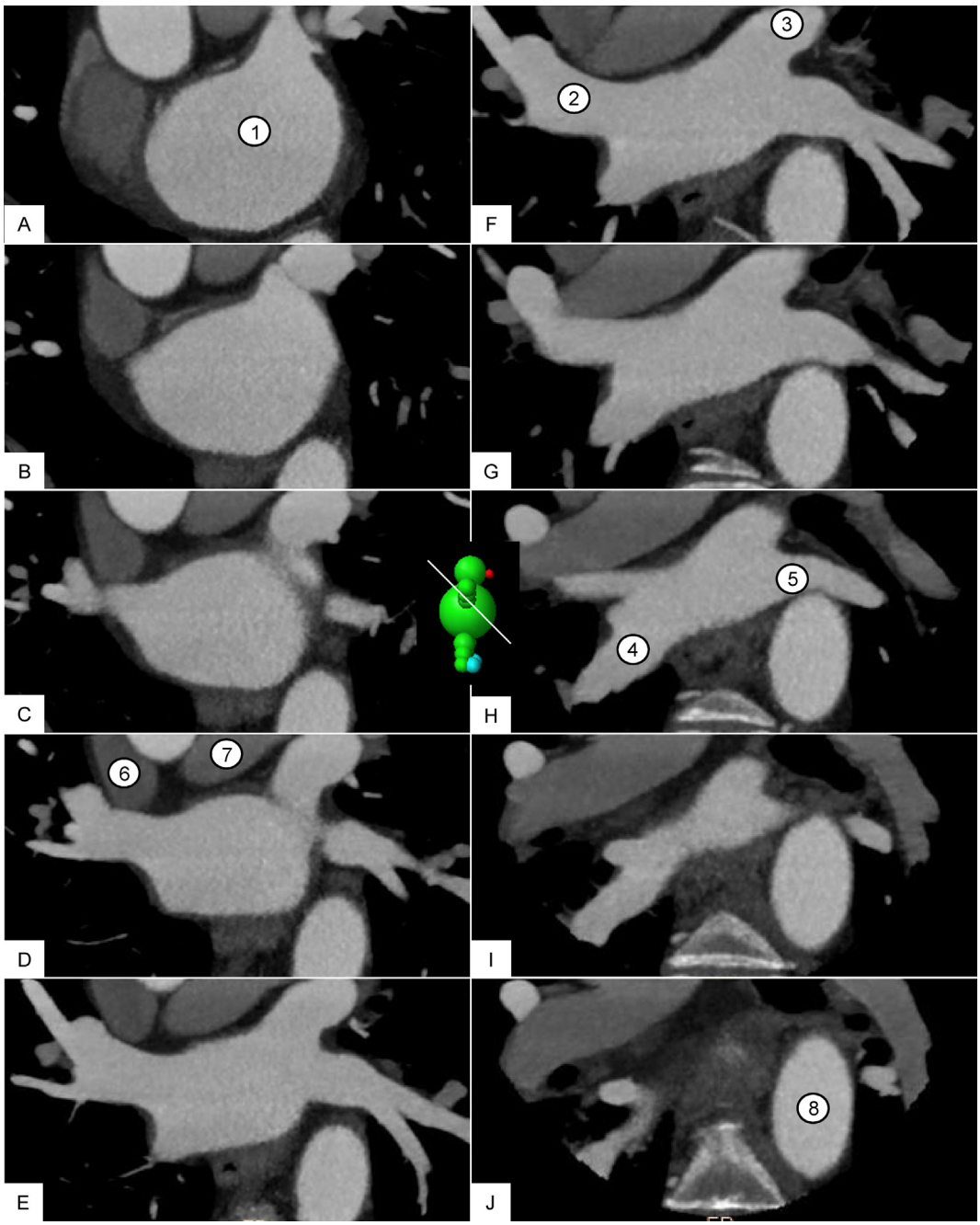

Fig. 2. Anatomy of the pulmonary veins on cardiac-gated contrast-enhanced computed tomography, viewed in a coronal oblique plane in a cardiology patient, moving from anterior (A) to posterior (J), with a central cartoon demonstrating the plane of view. *Left atrium; 2. Right superior pulmonary vein; 3. Left superior pulmonary vein; 4. Right inferior pulmonary vein; 5. Left inferior pulmonary vein; 6. Right main pulmonary artery; 7. Left main pulmonary artery; 8. Descending aorta).*

soidal and elliptical, as shown in Fig. 2. The use of software interpolation tools on treatment planning is not beneficial, given the considerable change in geometry between adjacent slices. Similarly, while the coronal and sagittal planes can be exploited for additional perspective when resolving difficult soft tissue boundaries on the axial plane, as the PVs are positioned obliquely, these planes of view are not always additive.

Region of interest derivation

Given that the myocardial sleeve tissue responsible for generating AF is a short 'central' portion of the vein, this was identified as the region of interest (ROI) for treatment planning purposes.

Whilst the average length of the anatomical pulmonary vein is up to 45 mm, the length of the vein that contains myocardial sleeve is constrained to the 20–25 mm central aspect of the vein, adjacent to the LA. The mid-point of this range (i.e. 23 mm) was therefore taken forward as a pragmatic PV-ROI length. In terms of the PV-ROI width, both the vein wall and the vein lumen are included, which radiologically has a diameter of 11 mm (see Fig. 2). The anatomical veins approach the LA at an angle of $\sim 25^{\circ}$ to the horizon, giving a maximum total superior-inferior height on axial CT of 21 mm approximately (10 mm as per **Supplementary** Fig. 1, plus 11 mm for vein diameter). It is recommended that the most superior/inferior 'edge' of a PV-ROI, where the lumen has partially merged with the LA, is contoured. These are often discernible by

Table 1
Cranio-caudal limits of the pulmonary veins on four-dimensional computed tomography radiotherapy plans, assuming 2.5 mm slice thickness.

	Right Superior Pulmonary Vein (RSPV) *Typically joins from the superolateral direction to the LA lateral wall.*	**Left Superior Pulmonary Vein (LSPV)** *Typically joins from superolateral direction to the LA 'roof'.*
Superior	One slice above the highest slice where the RSPV is in contact with the LA	Approximately 7 slices above the inferior limit.
Inferior	The lowest slice where the outline of the vein can be distinguished from the LA.	The lowest slice where the (elongated) oval shape of the vein is distinct.
	Right Inferior Pulmonary Vein (RIPV) *Typically joins from inferolateral direction to the LA lateral wall.*	**Left Inferior Pulmonary Vein (LIPV)** *Typically joins from the inferolateral direction to the posterolateral LA wall.*
Superior	The highest slice where the RIPV outline can be distinguished from the LA.	The highest slice where the LIPV outline can be distinguished from the LA.
Inferior	One slice below the lowest slice where the RIPV is first in contact with the LA.	One slice below the lowest slice where the LIPV is first in contact with the LA.

their protuberance and/or the altered attenuation of the intraluminal blood in contrast-enhanced studies.

Segmentation guidance

Prior to beginning PV segmentation, the wall and blood pool of the LA should be contoured without the auricle, according to the Milo atlas (18), resulting in an oval-shaped LA structure. A 'halo' structure should be created by duplicating the LA and growing this by a 23 mm margin isotropically, which will serve as a guide for the maximum PV-ROI length peripherally. A 5 mm roller-ball should be used to encompass all visible PV on axial slices within the halo, excluding small branches of a diameter less than the roller-ball. Accessory veins within the confines of the cranio-caudal limits outlined should be contoured if they are visible on $\geq$ 3 consecutive slices. Larger third (and fourth) veins should be included in either the superior or inferior structure, whichever they are most proximal to. It is recommended that 'mediastinal' window settings are utilised in the first instance (i.e. window width 350 HU, window level 50 HU), but others are acceptable depending on the presence and timing of intravenous contrast media.

The PV-ROI are contoured over approximately 21 mm cranio-caudally (e.g. eight axial CT slices at 2.5 mm thickness). If this height has not been contoured after following the vein-specific guidance in Table 1, the peripheral PV-ROI should be extended until 21 mm are reached, where possible. The use of less axial slices may be necessary due to early bifurcation into tiny or invisible branches, or because a vein courses towards the horizon peripherally. As it is important to encompass the PV-ROIs on all slices where it is contact with the LA, the use of more than eight slices (i.e. of 2.5 mm thickness) is also permitted.

In the event of the superior and inferior veins having a common region where they join the LA, the course of the two veins peripherally may guide where the boundary of the superior and inferior structures is placed. Finally, PV-ROIs should then be cropped outside the halo structure, and inside the LA structure, as shown in Fig. 3. An example of a contrast-enhanced case and an unenhanced case can be found as **Supplementary Files**.

Radiotherapy treatment plans

The datasets of five patients with locally advanced lung cancer receiving radiotherapy recently at our centre were randomly chosen for atlas evaluation. Patients were immobilised in the supine position using a knee rest and thorax board, with arms above their head holding a T-bar. Scans were completed during quiet respiratory motion using the Varian RPM system (Varian Medical Systems, Palo Alto, CA, USA) and the GE Advantage Sim 4D application (GE Medical Systems, Milwaukee, WI, USA). Ten phase bins were created in order to generate an average image intensity projection of the four-dimensional radiotherapy planning scan (4D-AVE), which was used for atlas evaluation. CT images at 2.5 mm slice thickness were acquired from the cricoid to the second lumbar vertebra with intravenous contrast when possible. Volumetric modulated arc therapy (VMAT) treatment plans were calculated using the Varian AAA 13.6.23 algorithm on the Varian Eclipse treatment planning system and are illustrated in Fig. 4. The dose prescriptions used in this cohort were 55 Gy in 20 fractions over four weeks, or 72 Gy in 40 fractions over 8 weeks.

Atlas evaluation

To formally assess the suitability of the proposed atlas, five clinical oncologists (JM, CH, GH, CC, KT) and two radiation technologists (SB, CN) without any prior experience or training in contouring the PVs were invited to demonstrate the atlas on the five clinical cases. The two example cases mentioned above were provided along with the atlas. Locally advanced lung cancer cases were selected from a local database on the basis of having significant lymphadenopathy and therefore considerable incidental dose coverage of at least one PV. Patients with pulmonary vein invasion were excluded. Patient, tumor and radiotherapy characteristics are available in **Supplementary Table 1**. The 4D-AVE was used for all segmentations, and an auto-segmented LA contour based was provided for the observers, which they were permitted to modify. The LA structure was an autosegmentation using the Haq tool (21), which is based on the Feng definitions (16), aligning with how contemporary treatment planning workflows are commonly furnished with automated tools for organs at risk including the cardiac substructures (22). Geometric and dosimetric comparisons of the observer structures were then made with reference structures previously jointly created by GW, CM and PB, using a range of metrics as per recommendations for inter-observer variation studies (23,24). Difference in volume (VD), centroid shift (CS), Dice similarity coefficient (DSC), and mean Hausdorff distance (HDM) were calculated using Slicer-RT (PerkLab, Ontario, Canada) (25). Whilst there is a lack of consensus on the optimal values for these metrics (23,24), a higher DSC (particularly $\geq$ 0.80) and lower VD, CS, HDM equate to better contour concordance (23,24). The dose metrics analysed were mean dose (MD) and maximum dose to 0.5 cc (Dmax) as per Eclipse calculations.

Statistical analysis

Following data collection, statistics were calculated using Prism v8.3.0 (GraphPad Software, San Diego, California, USA). Mean and standard deviations are displayed and were used for significance

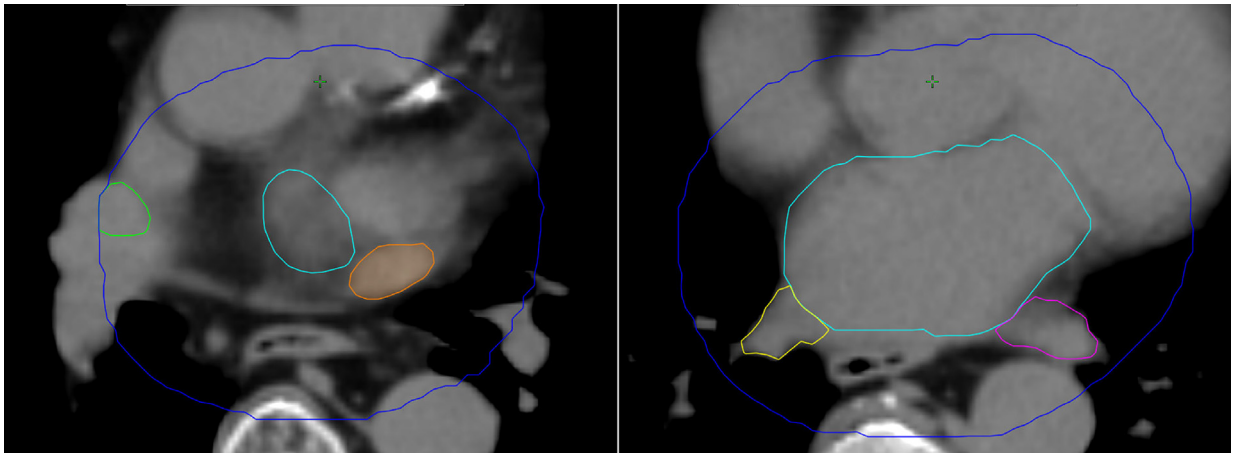

Fig. 3. Representative pulmonary vein anatomy of the left atrium (light blue) and the halo (dark blue) on an unenhanced axial CT slice, demonstrating how the right superior pulmonary vein is cropped by the halo peripherally and the right inferior vein is cropped centrally by the LA *(green = right superior pulmonary vein; yellow = right inferior pulmonary vein; orange = left superior pulmonary vein; purple = left inferior pulmonary vein).*

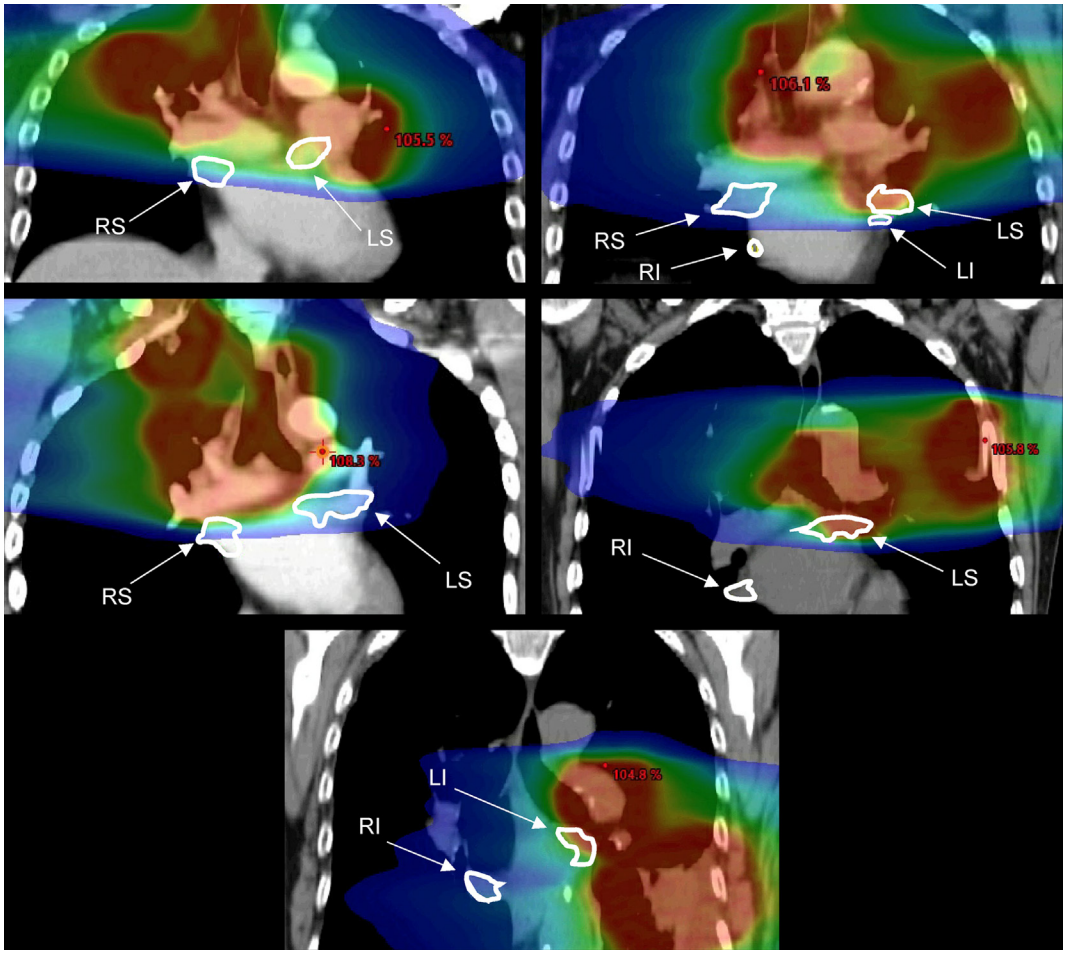

Fig. 4. Representative coronal average image projection slices from the four-dimensional computed tomography radiotherapy plans of the five included patients including pulmonary vein delineations (highlighted with white arrows) and the radiation dose distribution overlaid (*RS = right superior pulmonary vein; RI = right inferior pulmonary vein; LS = left superior pulmonary vein; LI = left inferior pulmonary vein*).

testing with t tests, as most data were normally distributed according to the Shapiro-Wilk test. Correlation between metrics was assessed with Pearson's coefficient. Exploratory analyses of the impact of relevant clinical factors included significance testing with the F statistic from repeated measures 2-way ANOVA (**Supplementary Tables 2–4**).

Results

Overall, the PVs were found to be small structures of mean volume 4.2 cc ± 1.5 in the reference contours. The superior PVs were consistently larger than the inferior PVs and the left-sided PVs were consistently larger than the right PVs, as shown in Supple-

mentary Table 5. The mean MD to the PVs was 35.0% ± 25 of the prescription dose in the five locally advanced NSCLC cases tested, and the mean Dmax was 61% ± 37 (see Supplementary Table 5).

Contour overlap with the reference structures was fair overall, with a mean DSC 0.80 ± 0.02 across all PVs. The RSPV (mean DSC 0.83 ± 0.02) had better overlap than the LSPV (mean DSC 0.80 ± 0.03), but the inferior PVs were equivalent, both having a mean DSC of 0.78, as shown in Fig. 5A. Similarly, VD (mean 0.46 cc ± 0.19 (16%)) and centroid shifts (2.5 mm) were small overall, with the worst performance being for the LIPV (0.57 cc ± 0.62, 2.9 mm ± 0.88), and the best for the RIPV (0.17 cc ± 0.40, 2.57 mm ± 0.71) (see Fig. 5B-C).

The mean magnitude of directional shifts was 1.8 mm and shifts in the right-left axis were equally balanced in direction. Shifts in the cranio-caudal and dorso-ventral axes were in the one direction only however (posterior and superior respectively). HDM values were also low generally (see Fig. 5D), and the RSPV delineation was the most optimal according to this metric (HDM 0.97 mm ± 0.14). Consistent trends were apparent across multiple PVs for the same observer for some geometric parameters (e.g. centroid shift for △).

Differences in MD and Dmax between the observer and reference structures were generally very low (overall mean MD difference 0.79 Gy ± 0.71 (1.46% ±1.25); overall mean Dmax difference 0.28 Gy ± 1.36 (0.58% ±2.41). The lowest dose differences were exhibited for RIPV, with a mean MD difference of −0.23 Gy ± 0.28 and mean Dmax difference of −0.65 Gy ± 1.08. The highest difference for MD was for the LSPV (1.43 Gy ± 0.64) and for Dmax, the LIPV (Dmax 2.05 Gy ± 3.05), as shown in Fig. 5E-F. There was a trend for larger dose differences corresponding with larger volume differences for a very limited number of particular observers on specific PVs (e.g. LIPV for ■ and ● observers). There was little correlation between DSC and dose differences however, as shown in Supplementary Table 6.

Discussion

In this study, a guide for contouring the PVs on RT planning scans was developed via the combined clinical expertise of radiology, cardiology and oncology. Whilst radiation oncologists exercise caution in thoracic cases with implanted cardiac devices and increasingly seek to reduce mean heart dose, incidental dose received by the PVs is not given specific consideration during treatment planning. As multiple retrospective studies have noted an elevated risk of arrhythmia following thoracic radiotherapy (1–6), dedicated substructure dosimetry studies with a standardised approach to PV definition, are urgently indicated.

The presented PV atlas led to consistent contours when applied by seven observers to five locally advanced lung cancer cases, as evidenced by high geometric similarity and low dosimetric differences compared to reference structures. The PVs were each contoured with similar degrees of success, with no agreement found between the geometric parameters regarding the best performing PV. Interestingly, in exploratory analyses for which the study was not specifically powered, atlas performance was not significantly impacted by the absence of intravenous contrast, or the presence of complex anatomical variations (**Supplementary File**).

PV delineation can be challenging as the four PVs have distinct morphologies, lack definitive boundaries with the LA, exhibit high degrees of inter-patient anatomical variation and are subject to motion artefact from cardiorespiratory movement. It would not be possible to encompass all of these factors in a user-friendly atlas, but the guidance presented provides basic principles. Observer accuracy metrics compared favourably to the other atlases in the cardiac substructure field (16–20). For example, the mean DSCs reported by Socha et al for a cardiac valve atlas ranged between 0.45 and 0.69, and HDMs were > 2 mm (20), whereas in this study, mean DSCs ranged between 0.78 and 0.83, and HDMs ≤ 1.1 mm. As such atlas validation studies typically demonstrate lower concordance for small structures (16,17), the results presented are better than anticipated.

In alignment with the geometric parameters, the mean dose differences between observers and the reference contours were small, 0.79 Gy for mean dose and 0.28 Gy for Dmax. These are better than previous coronary artery atlas development studies (16). Poor correlation was observed between DSC and the dose differences may be explained by high-dose region edges occurring near the PVs due to the presence of mediastinal lymph nodes proximal to the superior heart (Fig. 4).

Ultimately, given their geometric complexity, the PV structures may be best generated by automated means in the future, as the performance of auto-segmentation algorithms improve (26). The atlas presented could play an important role in building the training datasets with the manual structures required for the development of such algorithms. In the interim, exploratory analyses on this dataset suggest the atlas is accessible to both clinicians and non-clinical staff, which is important as radiotherapy teams diversify and delegate specialised skills such as contouring to non-medical roles (27).

Large retrospective thoracic radiation datasets with PV structures are required to elicit the tolerance of the PVs for arrhythmia endpoints. Adherence to a uniform contouring atlas, or high-performing algorithm, for the PVs will conceivably enable researchers to clinically determine the other radiobiological characteristics of the PVs too, such as the tissue organisation model. Individual PVs may be classified as mixed 'serial'-'parallel' organs, since multiple 'chains' of cardiomyocytes in the myocardial sleeve ordinarily act to rapidly conduct electric potentials simultaneously. Alternatively, as a high maximum dose to a single point within any of the four PVs could theoretically result in sufficient focal myofibril disorganisation or interstitial fibrosis to form an arrhythmogenic substrate, a 'serial' model is perhaps more appropriate overall.

Of note, the four PVs are not equally accountable for the burden of AF presenting to the general cardiology department (28). A complete consensus is lacking but clinical electrophysiology studies suggest that the superior PVs more commonly contain arrhythmogenic tissue, and that the right PVs are more commonly implicated also. Whether this association remains true in the setting of radiotherapy should be factored into the design of future radiation oncology studies. Separate analyses of bilateral (i.e. RSPV + LSPV, RIPV + LIPV) and unilateral (i.e. RSPV + RIPV, LSPV + LIPV) combinations of PVs, as well as individual structures, and a composite, 'all_PVs' volume are warranted. Single PV studies may also be informative, both from an academic perspective, and clinically, given the ultracentral SABR is likely to be offered to select patients with lung tumours in the future.

Recent data report that dose to the sino-atrial node (SAN) and atrial chambers are associated with AF (29). The SAN is a region of right atrial wall myocardium that is responsible for initiating each cardiac depolarisation. An atlas for contouring this structure and the related atrioventricular node, for which there is no clinical data at present, was published recently (19). However given that the vast majority of AF ectopic foci originate in the PVs, which are located close to the atria and SAN, future studies should compare their relative dosimetric impact.

Crucially, in applying the presented atlas to interrogate the relationship between PV dose-volume metrics and arrhythmia outcomes, the inclusion of relevant clinical factors such as cardiac history, cardiovascular drugs and atrial dimensions has merit also

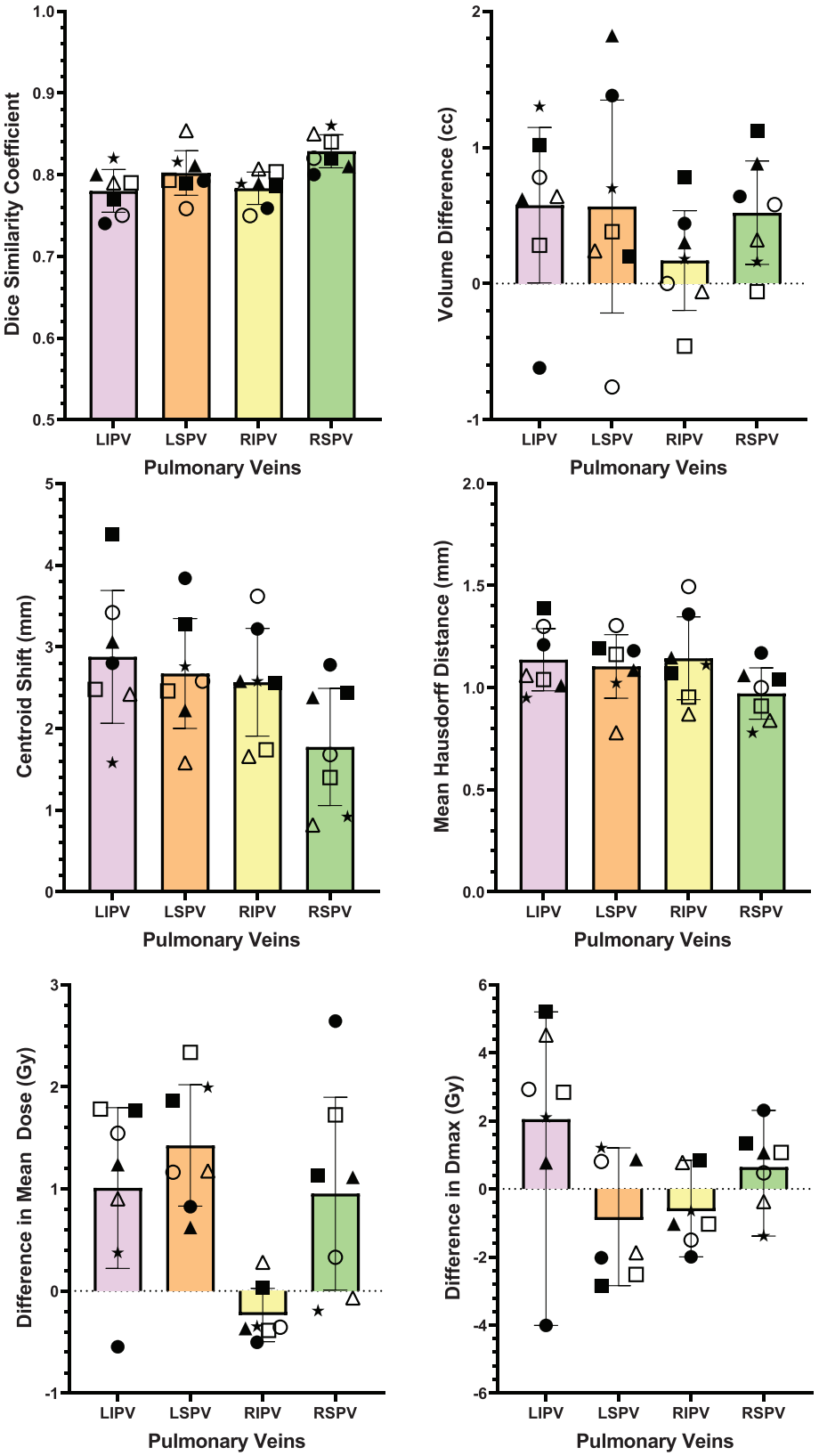

Fig. 5. Comparison of observer contour geometry (A-D) and dosimetry (E-F) metrics between reference contours and 7 observers (represented by different symbols) *(LIPV = left inferior pulmonary vein (purple); LSPV = left superior pulmonary vein (orange); RSPV = right superior pulmonary vein (green); RIPV = right inferior pulmonary vein (yellow)).*

(30), as AF is common in patients without cancer and those receiving extrathoracic radiotherapy (31).

The strengths of this study include the multi-faceted and multidisciplinary nature of the atlas' development, the use of contemporary radiotherapy plans for evaluation, and the inclusion of an interdisciplinary assessment. The study was designed using the principles and framework laid out by Vinod and colleagues (23). The main limitations of this study are the relatively small number of radiotherapy datasets and observers that testing was undertaken with, although these commensurate with other cardiac atlas development studies. In particular, small sample size restricts the interpretation of the exploratory analyses.

Aligning with the international effort to refine stereotactic ablative radiotherapy (SABR) as a treatment for tachycardia arising from the cardiac ventricles, recent pre-clinical research has demonstrated the application of SABR as a treatment for AF (32–34). In cardiology, intentional induction of widespread fibrosis at the PV-LA boundaries with invasive radiofrequency ablation to electrically isolate aberrant tissue in PVs is the current standard-of-care for refractory AF, for a select population. A feasibility study using SABR to treat AF suggested this approach is effective and safe (35). As arrhythmogenic foci are commonly found at multiple PV-LA junctions in AF, invasive radiofrequency ablations typically involve the entire PV region, which has been shown to be feasible with SABR fields in a multimodality planning study (36). A phase II clinical trial testing uniform treatment to all four PV regions has recently launched and will provide preliminary safety and efficacy signals (37). The dimensions and limits of the PV targets for AF SABR treatments have not been defined in any of the clinical or pre-clinical literature to date, therefore this atlas may inform future cardiac SABR research also.

Ultimately, clinical dosimetric studies of consistently contoured PVs could facilitate the derivation of safe dose thresholds below which radiotherapy-related arrythmia is unlikely in thoracic treatment. Furthermore, the atlas outlined may also have research applications in the evolving field of SABR for cardiac arrhythmia, in providing guidance for uniform targeting of the PVs.

Conclusion

Recommendations for consistent delineation of the PVs were prepared by a multidisciplinary group of clinicians based on the available histological and radiological literature and integrated clinical expertise. This atlas should serve as a basis for standardised radiotherapy PV dosimetry studies examining arrhythmia endpoints.

Declaration of Competing Interest

The authors declare that they have no known competing financial interests or personal relationships that could have appeared to influence the work reported in this paper.

Acknowledgment

This work was performed within the Irish Clinical Academic Training (ICAT) Programme, supported by the Wellcome Trust and the Health Research Board (Grant Number 203930/B/16/Z), the Health Service Executive National Doctors Training and Planning and the Health and Social Care, Research and Development Division, Northern Ireland. None of the the funders had any role in the conduct of the research.

Appendix A. Supplementary material

Supplementary data to this article can be found online at https://doi.org/10.1016/j.radonc.2023.109680.

References

[1] Hotca A, Thor M, Deasy JO, Rimner A. Dose to the cardio-pulmonary system and treatment-induced electrocardiogram abnormalities in locally advanced non-small cell lung cancer. Clin Transl Radiat Oncol 2019;19:96–102.
[2] Vivekanandan S, Landau DB, Counsell N, Warren DR, Khwanda A, Rosen SD, et al. The impact of cardiac radiation dosimetry on survival after radiation therapy for non-small cell lung cancer. Int J Radiat Oncol Biol Phys 2017;99:51–60.
[3] Gomez DR, Yusuf SW, Munsell MF, Welsh JW, Liao Z, Lin SH, et al. Prospective exploratory analysis of cardiac biomarkers and electrocardiogram abnormalities in patients receiving thoracic radiation therapy with high-dose heart exposure. J Thorac Oncol Off Publ Int Assoc Study Lung Cancer 2014 Oct;9:1554–60.
[4] Cai G, Li C, Yu J, Meng X. Heart dosimetric parameters were associated with cardiac events and overall survival for patients with locally advanced esophageal cancer receiving definitive radiotherapy. Front Oncol 2020;10:1–13.
[5] Ogino I, Watanabe S, Iwahashi N, Kosuge M, Sakamaki K, Kunisaki C, et al. Symptomatische strahleninduzierte Herzerkrankung bei Langzeitüberlebenden nach Ösophaguskarzinom. Strahlenther Onkol 2016;192:359–67.
[6] Konski A, Li T, Christensen M, Cheng JD, Yu JQ, Crawford K, et al. Symptomatic cardiac toxicity is predicted by dosimetric and patient factors rather than changes in 18F-FDG PET determination of myocardial activity after chemoradiotherapy for esophageal cancer. Radiother Oncol 2012;104:72–7.
[7] Fradley MG, Beckie TM, Brown SA, Cheng RK, Dent SF, Nohria A, et al. Recognition, prevention, and management of arrhythmias and autonomic disorders in cardio-oncology a scientific statement from the American Heart Association. Circulation 2020;E41–55.
[8] Bandyopadhyay D, Ball S, Hajra A, Chakraborty S, Dey AK, Ghosh RK, et al. Impact of atrial fibrillation in patients with lung cancer: insights from National Inpatient Sample. IJC Hear Vasc 2019;22:216–7.
[9] Yun JP, Choi EK, Do HK, Park SH, Jung JH, Park SH, et al. Risk of atrial fibrillation according to cancer type: a nationwide population-based study. JACC Cardio Oncol 2021;3:221–32.
[10] Apte N, Dherange P, Mustafa U, Ya'qoub L, Dawson D, Higginbotham K, et al. Cancer Radiation Therapy May Be Associated With Atrial Fibrillation. Front Cardiovasc Med. 2021;8:1–9.
[11] Khan R. Identifying and understanding the role of pulmonary vein activity in atrial fibrillation. Cardiovasc Res 2004;64:387–94.
[12] Chard M, Tabrizchi R. The role of pulmonary veins in atrial fibrillation: a complex yet simple story. Pharmacol Therapeut 2009;124:207–18.
[13] Ellis CR, Saavedra P, Kanagasundram A, Estrada JC, Montgomery J, Farrell M, et al. Pulmonary vein sleeve length and association with body mass index and sex in atrial fibrillation. JACC Clin Electrophysiol 2018;4:412–4.
[14] Schwartzman D, Lacomis J, Wigginton WG. Characterization of left atrium and distal pulmonary vein morphology using multidimensional computed tomography. J Am College Cardiol 2003;41:1349–57.
[15] Walls GM, O'Kane R, Ghita M, Kuburas R, McGarry CK, Cole AJ, et al. Murine models of radiation cardiotoxicity: a systematic review and recommendations for future studies. Radiother Oncol 2022. in press.
[16] Feng M, Moran JM, Koelling T, Chughtai A, Chan JL, Freedman L, et al. Development and validation of a heart atlas to study cardiac exposure to radiation following treatment for breast cancer. Int J Radiat Oncol Biol Phys 2011;79:10–8.
[17] Duane F, Aznar MC, Bartlett F, Cutter DJ, Darby SC, Jagsi R, et al. A cardiac contouring atlas for radiotherapy. Radiother Oncol 2017;122:416–22.
[18] Milo MLH, Offersen BV, Bechmann T, Diederichsen ACP, Hansen CR, Holtved E, et al. Delineation of whole heart and substructures in thoracic radiation therapy: National guidelines and contouring atlas by the Danish Multidisciplinary Cancer Groups. Radiother Oncol 2020;150:121–7.
[19] Loap P, Servois V, Dhonneur G, Kirov K, Fourquet A, Kirova Y. A radiation therapy contouring atlas for cardiac conduction node delineation. Pract Radiat Oncol 2021;11:e434–7.
[20] Socha J, Rygielska A, Uziębło-Życzkowska B, Chałubińska-Fendler J, Jurek A, Maciorowska M, et al. A heart valves contouring atlas on average intensity projection 4D-CT for lung cancer radiotherapy. Radiother Oncol 2021;161:S975–7.
[21] Haq R, Hotca A, Apte A, Rimner A, Deasy JO, Thor M. Cardio-pulmonary substructure segmentation of radiotherapy computed tomography images using convolutional neural networks for clinical outcomes analysis. Phys Imaging Radiat Oncol 2020;14:61–6.
[22] Walls GM, Giacometti V, Apte A, Thor M, McCann C, Hanna GG, et al. Validation of an established deep learning auto-segmentation tool for cardiac substructures in 4D radiotherapy planning scans. Phys Imaging Radiat Oncol 2022. in press.

[23] Vinod SK, Jameson MG, Min M, Holloway LC. Uncertainties in volume delineation in radiation oncology: a systematic review and recommendations for future studies. Radiother Oncol 2016;121:169–79.
[24] Hanna GG, Hounsell AR, O'Sullivan JM. Geometrical analysis of radiotherapy target volume delineation: a systematic review of reported comparison methods. Clin Oncol (R Coll Radiol) 2010 Sep;22:515–25.
[25] Pinter C, Lasso A, Wang A, Jaffray D, Fichtinger G. SlicerRT: radiation therapy research toolkit for 3D Slicer. Med Phys 2012 Oct;39:6332–8.
[26] Sherer MV, Lin D, Elguindi S, Duke S, Tan LT, Cacicedo J, et al. Metrics to evaluate the performance of auto-segmentation for radiation treatment planning: a critical review. Radiother Oncol 2021;160:185–91.
[27] Duffton A, Moore K, Williamson A. Diversity in radiation therapist/therapeutic radiographer (RTT) advanced practice (AP) roles delivering on the four domains. Tech Innov Patient Support Radiat Oncol 2021;17:102–7.
[28] Kistler PM, Roberts-Thomson KC, Haqqani HM, Fynn SP, Singarayar S, Vohra JK, et al. P-wave morphology in focal atrial tachycardia: development of an algorithm to predict the anatomic site of origin. J Am Coll Cardiol 2006;48:1010–7.
[29] Kim KH, Oh J, Yang G, Lee J, Kim J, Gwak S, et al. Association of sinoatrial node radiation dose with atrial fibrillation and mortality in patients with lung cancer. JAMA Oncol 2022 Sep 22.
[30] Atkins K, Nikolova A, Guthier C, Bitterman D, Kozono D, Nohria A, et al. Association of Cardiac Sub-Structure Radiation Dose with Bradyarrhythmias and Tachyarrhythmias after Lung Cancer Radiotherapy. In: International Journal of Radiation Oncology Biology Physics. 2022. p. 358: 202.
[31] Bucknell NW, Belderbos J, Palma DA, Iyengar P, Samson P, Chua K, et al. Avoiding toxicity with lung radiation therapy: an IASLC perspective. J Thorac Oncol 2022.
[32] Bode F, Blanck O, Gebhard M, Hunold P, Grossherr M, Brandt S, et al. Pulmonary vein isolation by radiosurgery: implications for non-invasive treatment of atrial fibrillation. Europace 2015;17:1868–74.
[33] Zei PC, Wong D, Gardner E, Fogarty T, Maguire P. Safety and efficacy of stereotactic radioablation targeting pulmonary vein tissues in an experimental model. Hear Rhythm 2018 Sep;15:1420–7.
[34] Chang JH, Cha MJ, Seo JW, Kim HJ, Park SY, Kim BH, et al. Feasibility study on stereotactic radiotherapy for total pulmonary vein isolation in a canine model. Sci Rep 2021;11:1–9.
[35] Qian PC, Azpiri JR, Assad J, Gonzales Aceves EN, Cardona Ibarra CE, de la Pena C, et al. Noninvasive stereotactic radioablation for the treatment of atrial fibrillation: first-in-man experience. J Arrhythmia 2020;36:67–74.
[36] Ren XY, He PK, Gao XS, Zhao ZL, Zhao B, Bai Y, et al. Dosimetric feasibility of stereotactic ablative radiotherapy in pulmonary vein isolation for atrial fibrillation using intensity-modulated proton therapy. J Appl Clin Med Phys 2021;22:79–88.
[37] Di Monaco A, Gregucci F, Bonaparte I, Troisi F, Surgo A, Di Molfetta D, et al. Paroxysmal Atrial Fibrillation in Elderly: Worldwide Preliminary Data of LINAC-Based Stereotactic Arrhythmia Radioablation Prospective Phase II Trial. Front Cardiovasc Med. 2022;9.